# Direction of Arrive Estimation in Spherical Harmonic Domain Using Super Resolution Approach

Jie Pan(✉), Yalin Zhu, and Changling Zhou

College of Information Engineering, Yangzhou University,
Yangzhou 221000, China
panjie1982@nuaa.edu.cn

**Abstract.** Spherical array plays important role in 3D targets localization. In this paper, we develop a novel DOA estimation method for the spherical array with super resolution approach. The proposed method operates in spherical harmonic domain. Based on the atomic norm minimization, we develop a gridless L1-SVD algorithm in spherical harmonic domain and then we adopt the spherical ESPRIT method to two-dimensional DOA estimation. Compared to the previous work, the proposed method acquires better estimation performance. Numerical simulation results verify the performance of the proposed method.

**Keywords:** DOA estimation · Spherical harmonics · Atomic norm

## 1 Introduction

Direction-of-arrive (DOA) estimation is an attractive topic in array signal processing and finds a variety of application in acoustics and radio science [1]. In recent years, spherical array has received much attention because of the 3D array geometry configuration to estimation the azimuth and elevation of sources. The spherical array samples the wave-field by sensors distributed on a sphere. The manifold of the array can be transformed into Spherical Harmonic (SH) domain and analyze the wave-field with almost equal resolution in all directions [2, 3].

Several DOA estimation algorithms have been proposed in SH domain. In [4], conventional MUSIC method is implemented in terms of SH and ESPRIT method is extended for spherical array, called EB-ESPRIT, in [5]. In [6], the unitary transformations are proposed in real SH domain to reduce the computational complexity. Most of these methods rely on the spatial covariance matrix which decomposes the spatial covariance matrix into signal and noise subspace. However, in limited number of snapshots and coherent sources cases, the spatial covariance matrix will be distorted.

In [7], a discrete sparse recovery approach called variational sparse Bayesian learning (VSBL) is applied to SH domain. However, this approach needs discretizing the parameter space of interest with a grid and in practice the targets may locate off-grid. To alleviate this drawback, the off-grid sparse Bayesian inference (OGSBI) is extended to SH domain in [8], but this method is computationally prohibitive because of joint parameters optimization.


X. Gu et al. (Eds.): MLICOM 2017, Part II, LNICST 227, pp. 179–187, 2018.
https://doi.org/10.1007/978-3-319-73447-7_21

Recently, several works on sparse recovery have been proposed to estimate parameters with continuous value. In [9], Candès develops a mathematical theory of continuous sparse recovery for 1-D frequency extrapolation which called Super Resolution approach. In [10] Candès' method is utilized to DOA estimation for spatial coprime arrays. In [11], an alternative discretization-free sparse DOA estimation method for linear array is proposed. In [12, 13], covariance domain DOA estimation methods with continuous sparsity approach are developed. In [14, 15] the continuous sparse recovery approach for 1-D parameters is extended to 2-D frequency models.

These methods mentioned above utilize the Vandermonde structure of the sampled data so as to be limited in case of linear or rectangular arrays. Mahata extend the super resolution approach to arbitrary linear array and planar array for 1-D parameter estimation in [16, 17] respectively. However, to the best of author's knowledge, super resolution approach in SH domain is not available in literature.

In this paper, we propose a novel 2-D DOA estimation method in SH domain with super resolution approach. We reformulate the array manifold in SH domain as a weighted Vandermonde structure matrix. By utilizing this model, we modify the atomic norm minimization algorithm to adapt the processing in SH domain and estimate azimuth and elevation of targets by spherical ESPRIT. The proposed method do not need predefined dense grid and joint parameters optimization. Simulation results show the improved performance of the proposed method.

Notations: $(\bullet)^{\mathrm{T}}$ denote the transpose, $(\bullet)^{\dagger}$ denote pseudo inverse of a matrix and $(\bullet)^{\mathrm{H}}$ denote conjugate transpose of a matrix or vector. $vec(\bullet)$ denotes the vectorization operator and $diag(\boldsymbol{x})$ denotes a diagonal matrix. $\|\bullet\|_2$ denotes the Euclidean $l_2$ norm of a vector. $\otimes$ denotes the Kronecker product.

## 2 Signal Model

There is a spherical array with $I$ omnidirectional elements distributed on a sphere whose radius is $R$. The $i$th sensor is located at $\boldsymbol{r}_i = (R, \boldsymbol{\Phi}_i)$, where $\boldsymbol{\Phi}_i = (\theta_i, \varphi_i)$. There are $L$ narrowband far-field sources with wavenumber $k = \lambda/2\pi$ are imping the spherical array, where $\lambda$ is the wavelength of the sources. The $l$th source location is defined as $\boldsymbol{\Psi}_l = (\theta_l, \varphi_l)$, where $\theta$ is defined as elevation angle and $\varphi$ is defined as azimuth respectively. The received signals of sensors can be described as:

$$\boldsymbol{X}(t) = \boldsymbol{A}(\boldsymbol{\Psi})\boldsymbol{s}(t) + \boldsymbol{N}(t). \tag{1}$$

where $\boldsymbol{X}(t) = [x_1(t), \cdots, x_I(t)]^{\mathrm{T}}$ is the received data of sensors, $\boldsymbol{s}(t) = [s_1(t), \cdots, s_L(t)]^{\mathrm{T}}$ is the emitting signal by sources, and $\boldsymbol{n}(t)$ is additive Gaussian white noise and $E\{\boldsymbol{n}(t)\boldsymbol{n}^{\mathrm{H}}(t)\} = \sigma^2\boldsymbol{I}$.

$\boldsymbol{A}(\boldsymbol{\Psi}) = [\boldsymbol{a}(\boldsymbol{\Psi}_1), \cdots, \boldsymbol{a}(\boldsymbol{\Psi}_L)] \in \mathbb{C}^{I\times L}$ is the element-space manifold of the spherical array, where $\boldsymbol{a}(\boldsymbol{\Psi}_l) = [a_1(\boldsymbol{\Psi}_l), \cdots, a_I(\boldsymbol{\Psi}_l)]^{\mathrm{T}} \in \mathbb{C}^{I\times 1}$. The $i$th element of the steering vector $a_i(\boldsymbol{\Psi}_l)$ can be represented in SH series as:

$$a_i(\boldsymbol{\Psi}_l) = \sum_{n=0}^{N} \sum_{m=-n}^{n} b_n(kR)[Y_n^m(\boldsymbol{\Psi}_l)]^{\mathrm{H}} Y_n^m(\boldsymbol{\Phi}_i). \tag{2}$$

The far-field phase mode strength is given by:

$$b_n(kR) = \begin{cases} 4\pi i^n j_n(kR) & \text{open sphere} \\ 4\pi i^n (j_n(kR) - \frac{j_n'(kR)}{h_n'(kR)} h_n(kR)) & \text{rigid sphere} \end{cases}. \tag{3}$$

In (3), $h_n$ is spherical Hankel function of second kind and $j_n$ is spherical Bessel function of first kind. $j_n'$ and $h_n'$ are derivatives of $j_n$ and $h_n$. $Y_n^m(\theta, \varphi)$ is the $n$th order and $m$th degree spherical harmonic function:

$$Y_n^m(\theta, \varphi) = \sqrt{\frac{(2n+1)(n-m)!}{4\pi(n+m)!}} P_n^m(\cos\theta) e^{jm\varphi} \quad \forall 0 \le n \le N,\ 0 \le m \le n. \tag{4}$$

where $P_n^m(\cos\theta)$ is the associated Legendre polynomial.

It is shown in [5] that for order $n > kR$, the phase mode coefficient $b_n(kR)$ decrease super-exponentially. Hence, for the high order $n$ the phase mode $b_n(kR)$ will become small enough that we can truncate the steering vector in (2) to a limited order $N$ with tolerable error.

Consider maximum order $N$, substituting (2) into (1), the array manifold of the spherical array can be written as:

$$\boldsymbol{A}(\boldsymbol{\Psi}) = \boldsymbol{Y}(\boldsymbol{\Phi}) \boldsymbol{B}(kR) \boldsymbol{Y}^{\mathrm{H}}(\boldsymbol{\Psi}) \tag{5}$$

where $\boldsymbol{Y}(\boldsymbol{\Phi}) \in \mathbb{C}^{I \times (N+1)^2}$ is a spherical harmonic matrix. Its $i$th row vector can be given as:

$$\boldsymbol{y}(\boldsymbol{\Phi}_i) = [Y_0^0(\boldsymbol{\Phi}_i), Y_1^{-1}(\boldsymbol{\Phi}_i), Y_1^0(\boldsymbol{\Phi}_i), Y_1^1(\boldsymbol{\Phi}_i), \cdots, Y_N^N(\boldsymbol{\Phi}_i)]. \tag{6}$$

$\boldsymbol{Y}(\boldsymbol{\Psi})$ has the similar structure with (6). $\boldsymbol{B}(kR) \in \mathbb{C}^{(N+1)^2 \times (N+1)^2}$ is the mode strength matrix defined as:

$$\boldsymbol{B}(kR) = diag(b_0(kR), b_1(kR), b_1(kR), b_1(kR), \cdots, b_N(kR)) \tag{7}$$

Considering that the spherical harmonics are the orthonormal basis on unit 2-sphere, the spherical harmonics decomposition of the received data $\boldsymbol{X}(t)$ can be written as:

$$\boldsymbol{P}_{nm}(t) = \boldsymbol{Y}^{\mathrm{H}}(\boldsymbol{\Phi}) \boldsymbol{\Gamma} \boldsymbol{X}(t) \tag{8}$$

where $\boldsymbol{P}_{nm} = [P_{00}\, P_{1(-1)}\, P_{10}\, P_{11} \cdots P_{NN}]^{\mathrm{T}}$ and $\boldsymbol{\Gamma} = diag(\alpha_1, \alpha_2, \cdots, \alpha_I)$ is the weight matrix. For some special configurations of the spherical array and corresponding weight $\boldsymbol{\Gamma}$ introduced in [19], the spherical harmonic functions satisfy the orthogonality property:

$$\boldsymbol{Y}^{\mathrm{H}}(\boldsymbol{\Phi})\boldsymbol{\Gamma}\boldsymbol{Y}(\boldsymbol{\Phi}) = \boldsymbol{I} \tag{9}$$

Substituting (1) and (5) into (8), utilizing (9), the SH domain signal model can be written as:

$$\boldsymbol{P}_{nm}(t) = \boldsymbol{B}(kR)\boldsymbol{Y}^{\mathrm{H}}(\boldsymbol{\Psi})\boldsymbol{s}(t) + \boldsymbol{V}_{nm}(t) \tag{10}$$

where $\boldsymbol{V}_{mn}(t) = \boldsymbol{Y}^{\mathrm{H}}(\boldsymbol{\Phi})\boldsymbol{\Gamma}\boldsymbol{N}(t)$.

It is worth to note that the data model in SH domain can be described in weighted trigonometric polynomial form. This property will be useful for employing the super resolution approach in SH domain.

Considering the definition of the spherical harmonic function in (4), $P_n^m(\cos\theta)$ takes form of:

$$P_n^m(\cos\theta) = (\sin\theta)^{|m|} L_n^{(m)}(\cos\theta) \tag{11}$$

where $L_n^{(m)}$ is the $k$th derivative of the Legendre polynomial of degree $n$. Since $\cos\theta = (e^{j\theta} + e^{-j\theta})/2$ and $\sin\theta = (e^{j\theta} - e^{-j\theta})/2$, $P_n^m(\cos\theta)$ is a trigonometric polynomial of degree $n$ which is given by $P_n^m(\cos\theta) = \sum_{l=-n}^{n} \beta_{n,m,l} e^{jl\theta}$ with unique coefficients $\{\beta_{n,k,l}\}$. Then, we can write (4) as:

$$Y_n^m(\theta, \varphi) = \sum_{l=-n}^{n} A_{n.m}\beta_{n,m,l} e^{jl\theta} e^{jm\varphi} \tag{12}$$

where $A_{n.m} = \sqrt{\frac{(2n+1)(n-m)!}{4\pi(n+m)!}}$. Substituting (12) in (10), the SH domain data model can be given by:

$$\boldsymbol{P}_{nm} = \boldsymbol{B}(kR)\boldsymbol{G}\boldsymbol{D}(\boldsymbol{\Psi})\boldsymbol{s}(t) + \boldsymbol{V}_{nm}(t) \tag{13}$$

where $\boldsymbol{G} = [\boldsymbol{G}_{00}, \boldsymbol{G}_{1(-1)}, \boldsymbol{G}_{10}, \boldsymbol{G}_{11} \cdots \boldsymbol{G}_{NN}]^{\mathrm{T}}$, $\boldsymbol{G}_{mn} = [A_{n.m}\beta_{n,m,-n}, A_{n.m}\beta_{n,m,-(n-1)}, \cdots, A_{n.m}\beta_{n,m,n}]$, $\boldsymbol{D}(\boldsymbol{\Psi}) = [\boldsymbol{d}(\boldsymbol{\Psi}_1), \cdots, \boldsymbol{d}(\boldsymbol{\Psi}_L)]$, $\boldsymbol{d}(\boldsymbol{\Psi}_l)$ is written as:

$$\begin{aligned}
\boldsymbol{d}(\boldsymbol{\Psi}_l) &= \boldsymbol{d}_\theta(\theta_l) \otimes \boldsymbol{d}_\varphi(\varphi_l) \\
\boldsymbol{d}_\theta(\theta_l) &= \left[e^{-jN\theta_l}, \cdots, 1, \cdots, e^{jN\theta_l}\right]^{\mathrm{T}} \\
\boldsymbol{d}_\varphi(\varphi_l) &= \left[e^{-jN\varphi_l}, \cdots, 1, \cdots, e^{jN\varphi_l}\right]^{\mathrm{T}}
\end{aligned} \tag{14}$$

Considering the model described in (13) with $K$ snapshots, we stack them in a matrix as:

$$\boldsymbol{P} = \boldsymbol{B}(kR)\boldsymbol{G}\boldsymbol{D}(\boldsymbol{\Psi})\boldsymbol{S} + \boldsymbol{V} \tag{15}$$

where $\boldsymbol{P} = [\boldsymbol{P}_{nm}(t_1), \boldsymbol{P}_{nm}(t_2), \cdots, \boldsymbol{P}_{nm}(t_K)]$, $\boldsymbol{S} = [\boldsymbol{s}_1, \boldsymbol{s}_2, \cdots, \boldsymbol{s}_L]^{\mathrm{T}}$. The data model in (15) is utilized for the proposed SH domain DOA estimation method.

## 3 Super Resolution Approach in SH Domain

It is suggested in [12] that the noisy signal can be recovered by atomic norm minimization:

$$\begin{array}{ll} \min & \|\boldsymbol{Z}\|_A \\ s.t. & \|\boldsymbol{Z}-\boldsymbol{P}\| \leq \varepsilon \end{array} \tag{16}$$

where $A := \left\{\boldsymbol{B}(kR)\boldsymbol{G}\boldsymbol{d}(\Psi)\boldsymbol{s} | \Psi = (\theta, \varphi), \theta \in [0, \pi], \varphi \in [-\pi, \pi), \|\boldsymbol{s}\|_2 = 1\right\}$ denotes the atomic set. Due to L0-norm is not convex, we consider the convex relaxation and the atomic norm of $\boldsymbol{Z}$ which can be defined as:

$$\begin{aligned} \|\boldsymbol{Z}\|_A &= \inf\{t > 0 : \mathbf{Z} \in t \quad conv(A)\} \\ &= \inf\left\{ \sum\nolimits_l c_l \middle| \boldsymbol{Z} = \sum_l c_l \boldsymbol{B}(kR)\boldsymbol{G}\boldsymbol{d}(\boldsymbol{\Psi}_l)\boldsymbol{s}_l, c_l \geq 0 \right\} \end{aligned} \tag{17}$$

The conventional atomic norm minimization methods are relying on the Vandermonde decomposition of Toeplitz matrices, hence they are limited to Vandermonde structure model. Here, we utilize the relationship between the data model in SH domain and a Vandermonde matrix shown in (15) to develop an atomic norm minimization method in SH domain with semidefinite programing (SDP):

$$\begin{array}{ll} \min\limits_{\boldsymbol{T},\boldsymbol{W},\boldsymbol{Z}} & \frac{1}{2}\mathrm{tr}(S(\boldsymbol{T})) + \frac{1}{2}\mathrm{tr}(\boldsymbol{W}) \\ s.t. & \begin{bmatrix} S(\boldsymbol{T}) & \boldsymbol{Z} \\ \boldsymbol{Z}^{\mathrm{H}} & \boldsymbol{W} \end{bmatrix} \geq 0 \\ & \|\boldsymbol{B}(kR)\boldsymbol{G}\boldsymbol{Z} - \boldsymbol{P}\|_2 \leq \varepsilon \end{array} \tag{18}$$

where $\boldsymbol{T} \in \mathbb{C}^{(4N+1)\times(4N+1)}$, $S(\boldsymbol{T})$ is a two-fold block Toeplitz defined from $\boldsymbol{T}$ as:

$$S(\boldsymbol{T}) = \begin{bmatrix} \boldsymbol{T}_0 & \boldsymbol{T}_{-1} & \cdots & \boldsymbol{T}_{-2N} \\ \boldsymbol{T}_1 & \boldsymbol{T}_0 & \cdots & \boldsymbol{T}_{-2N+1} \\ \vdots & \vdots & \ddots & \vdots \\ \boldsymbol{T}_{2N} & \boldsymbol{T}_{2N-1} & \cdots & \boldsymbol{T}_0 \end{bmatrix} \tag{19}$$

where each block $\boldsymbol{T}_l, -2N < l < 2N$ is an $(2N+1) \times (2N+1)$ Toeplitz matrix constructed from the $l$th row of $\boldsymbol{T}$:

$$\boldsymbol{T}_l = \begin{bmatrix} x_{l,0} & x_{l,-1} & \cdots & x_{-2N} \\ x_{l,1} & x_{l,0} & \cdots & x_{l,-(2N-1)} \\ \vdots & \vdots & \ddots & \vdots \\ x_{2N} & x_{l,2N-1} & \cdots & x_{l,0} \end{bmatrix} \tag{20}$$

For the large number of snapshots $K$, we can factorize the matrix $\boldsymbol{P}$ in terms of singular value decomposition $\boldsymbol{P} = \boldsymbol{U\Sigma V}$, we can construct $\boldsymbol{P}' = \boldsymbol{U}_L\boldsymbol{\Sigma}_L$, where $\boldsymbol{\Sigma}_L$ is the diagram matrix consist of largest $L$ singular value and $\boldsymbol{U}_L$ is the corresponding singular value vectors. It is shown in [17] that the SDP problem in (18) can be written as:

$$\begin{aligned} \min_{\boldsymbol{T},\boldsymbol{W},\boldsymbol{Z}''} \quad & \tfrac{1}{2}\mathrm{tr}(S(\boldsymbol{T})) + \tfrac{1}{2}\mathrm{tr}(\boldsymbol{W}) \\ s.t. \quad & \begin{bmatrix} S(\boldsymbol{T}) & \boldsymbol{Z}'' \\ \boldsymbol{Z}''^{\mathrm{H}} & \boldsymbol{W} \end{bmatrix} \geq 0 \\ & \|\boldsymbol{B}(kR)\boldsymbol{G}\boldsymbol{Z}'' - \boldsymbol{P}'\|_2 \leq \varepsilon \end{aligned} \tag{21}$$

We argue that the choice of the parameter $\varepsilon$ can done as $\sqrt{LK\sigma^2}$. The proposed method in (21) can be regarded as the atomic norm minimization based L1-SVD algorithm in spherical harmonic domain.

Then, we can apply spherical ESPRIT [5] to the recovered covariance matrix $\boldsymbol{R} = \boldsymbol{B}(kR)\boldsymbol{G}S(\hat{\boldsymbol{T}})\boldsymbol{G}^{\mathrm{H}}\boldsymbol{B}^{\mathrm{H}}(kR)$ to estimate DOAs of the targets, where $S(\hat{\boldsymbol{T}})$ is the solution of (21). By expressing $\boldsymbol{R}$ in terms of eigenvalue decomposition, we can get:

$$\boldsymbol{R} = \boldsymbol{U}_s\boldsymbol{\Sigma}_s\boldsymbol{U}_s^{\mathrm{H}} + \sigma^2\boldsymbol{U}_N\boldsymbol{U}_N^{\mathrm{H}} \tag{22}$$

According to the property of the associated Legendre polynomials, the it can be given by:

$$\boldsymbol{D}_1\boldsymbol{U}_s^0 = \boldsymbol{E}\begin{bmatrix} \boldsymbol{\Delta}^T \\ \boldsymbol{\Delta}^H \end{bmatrix} \tag{23}$$

where $\boldsymbol{D}_1, \boldsymbol{D}_2, \boldsymbol{D}_3$ are auxiliary matrices with analytical expressions defined in [5], and $\boldsymbol{E}$ is given by:

$$\boldsymbol{E} = \begin{bmatrix} \boldsymbol{D}_2\boldsymbol{U}_s^{(-1)} & \boldsymbol{D}_3\boldsymbol{U}_s^{(1)} \end{bmatrix} \tag{24}$$

$\boldsymbol{U}_s^{(-1)}, \boldsymbol{U}_s^0, \boldsymbol{U}_s^{(1)}$ is the first, middle and last sub-matrix from $\boldsymbol{U}_s$ as shown in [5]. Then $\boldsymbol{\Delta}$ can be solved as:

$$\boldsymbol{\Delta} = (\boldsymbol{E}^H\boldsymbol{E})^{-1}\boldsymbol{E}^H\boldsymbol{D}_1\boldsymbol{U}_s^0 \tag{25}$$

Compute the eigenvalues $u_l, l = 1, 2, \cdots, L$ of $\boldsymbol{\Delta}$. The estimation of the elevation and azimuth of the $l$th target are $\theta_l = \tan^{-1}|u_l|$ and $\varphi_l = \arg(u_l)$ respectively.

## 4 Simulation Results

In this section, simulations are presented to study the DOA estimation performance of proposed method compared with the spherical ESPRIT in [5]. The radius $R$ of the spherical array used in the simulations is 0.042 m. There are 32 sensors mounted on the open sphere in a uniform way. The maximum order of the spherical harmonic is $N = 4$.

Firstly, we assume that there are two independent sources at $(\theta_1, \varphi_1) = (40^\circ, 70^\circ)$ and $(\theta_2, \varphi_2) = (50^\circ, 120^\circ)$ impinging the spherical array, where $\theta, \varphi$ are the elevation and azimuth respectively. 100 snapshots is collected. The RMSE of parameter estimation is defined as:

$$\text{RMSE} = \sqrt{\frac{1}{J}\sum_{j=1}^{J}(\widehat{\theta}_{ij} - \theta_i)} \tag{26}$$

$J$ the number of Monte Carlo trials is 200. The Fig. 1 shows that the proposed method achieve improved performance compared with the other methods especially in low SNR.

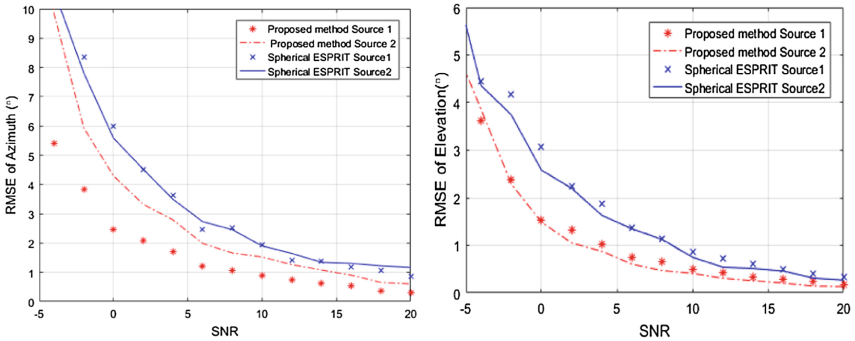


**Fig. 1.** RMSE of Azimuth and elevation versus SNR for uncorrelated sources

In the second example, we investigate the accuracy of our method in multipath environment. Considering two coherent sources at $(\theta_1, \varphi_1) = (40^\circ, 70^\circ)$ and $(\theta_2, \varphi_2) = (50^\circ, 120^\circ)$, SNR is 10 dB, the number of snapshot is 200. The number of Monte Carlo trials is 200. The simulation results of the proposed method and spherical ESPRIT are shown in Fig. 2.

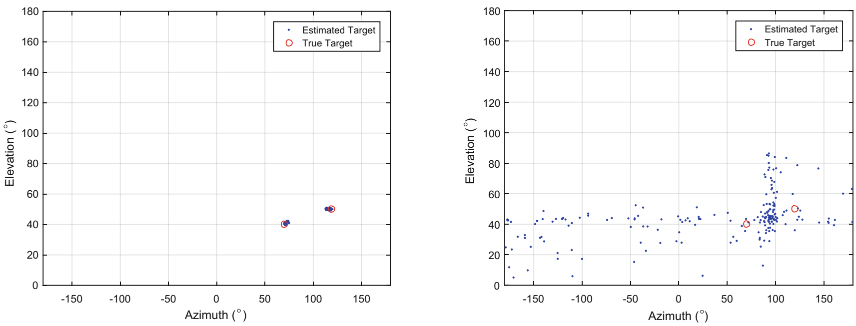


(a) Proposed Method (b) spherical ESPRIT

**Fig. 2.** Spectrum using different methods for coherent sources

It is shown that the proposed method works well with coherent sources, while the spherical ESPRIT method can't work in multipath environment.

## 5 Conclusions

In this paper, we proposed a novel DOA estimation method for spherical array with super resolution approach. The proposed method does not need the grid discretization and multiple parameters optimization. This method works well in low SNR and multipath environment. Simulations show our method the superior performance compared with conventional techniques.

**Acknowledgments.** This work was supported by National Natural Science Foundation of China (61601402), Jiangsu Province Science Foundation of China (BK20160477).

## References

1. Trees, H.L.V.: Optimum Array Processing: Part IV of Detection, Estimation and Modulation Theory. Wiley, New York (2002)
2. Teutsch, H., Kellermann, W.: Detection and localization of multiplewideband acoustic sources based on wavefield decomposition using spherical apertures. In: Proceedings of ICASSP 2008, pp. 5276–5279 (2008)
3. Rafaely, B., Peled, Y., Agmon, M., Khaykin, D., Fisher, E.: Spherical microphone array beamforming. In: Cohen, I., Benesty, J., Gannot, S. (eds.) Speech Processing in Modern Communication: Challenges and Perspectives, vol. 3. Springer, Berlin (2010). https://doi.org/10.1007/978-3-642-11130-3_11
4. Li, X., Yan, S., et al.: Spherical harmonics MUSIC versus conventional MUSIC. Appl. Acoust. **72**(9), 646–652 (2011)
5. Goossens, R., Rogier, R.: 2-D angle estimation with spherical arrays for scalar fields. IET Sig. Process. **3**(3), 221–231 (2009)
6. Huang, Q., Zhang, G., et al.: Unitary transformations for spherical harmonics MUSIC. Sig. Process. **131**, 441–446 (2016)
7. Huang, Q., Zhang, G., et al.: Real-valued DOA estimation for spherical arrays using sparse Bayesian learning. Sig. Process. **125**, 79–86 (2016)
8. Huang, Q., Xiang, L., et al.: Off-grid DOA estimation in real spherical harmonics domain using sparse Bayesian inference. Sig. Process. **137**, 124–134 (2017)
9. Candès, E.J., Fernandez-Granda, C.: Towards a mathematical theory of super-resolution. Commun. Pure Appl. Math. **67**(6), 906–956 (2014)
10. Tan, Z., Eldar, Y., et al.: Direction of arrival estimation using co-prime arrays: a super resolution viewpoint. IEEE Trans. Sig. Process. **62**(21), 5565–5576 (2014)
11. Yang, Z., Xie, L., et al.: A discretization-free sparse and parametric approach for linear array signal processing. IEEE Trans. Sig. Process. **62**(19), 4959–4973 (2014)
12. Hung, C.Y., Kaveh, M.: Super-resolution DOA estimation via continuous group sparsity in the covariance domain. In: IEEE International Conference on Acoustics, Speech and Signal Processing (2016)

13. Wu, X., Zhu, W.P., et al.: Direction-of-arrival estimation based on Toeplitz covariance matrix reconstruction. In: IEEE International Conference on Acoustics, Speech and Signal Processing (2016)
14. Tang, G., Bhaskar, B., Shah, P., Recht, B.: Compressed sensing off the grid. IEEE Trans. Inf. Theory **59**(11), 7465–7490 (2013)
15. Chi, Y., Chen, Y.: Compressive two-dimensional harmonic retrieval via atomic norm minimization. IEEE Trans. Sig. Process. **63**(4), 1030–1042 (2015)
16. Mahata, K., Hyder, M.M.: Frequency estimation from arbitrary time samples. IEEE Trans. Signal Process. **64**(21), 5634–5643 (2016)
17. Mahata, K., Hyder, M.M.: Grid-less TV minimization for DOA estimation. Sig. Process. **132**, 146–155 (2017)